Myeloid-derived Thrombospondin-1 contributes to abdominal aortic aneurysm through suppressing tissue inhibitor of metalloproteinases-1

Huan Yang[*,1], **Ting Zhou**[*,1], **Christine M. Sorenson**[3], **Nader Sheibani**[3], **Bo Liu**[#,1,2]

[1]Department of Surgery,School of Medicine and Public Health, University of Wisconsin-Madison, Madison, WI 53705

[2]Department of Cellular and Regenerative Biology, School of Medicine and Public Health, University of Wisconsin-Madison, Madison, WI 53705

[3]Department of Ophthalmology and Visual Sciences, University of Wisconsin-Madison, Madison, WI 53705

Abstract

OBJECTIVE: Abdominal aortic aneurysm (AAA) is characterized by the progressive loss of aortic integrity and accumulation of inflammatory cells primarily macrophages (Mφs). We previously reported that global deletion of matricellular protein thrombospondin-1 (TSP1) protects mice from aneurysm formation. The objective of the current study is to investigate the cellular and molecular mechanisms underlying TSP1's action in aneurysm.

APPROACH AND RESULTS: Using RNA fluorescent *in situ* hybridization, we identified Mφs being the major source of TSP1 in human and mouse aneurysmal tissues, accounting for over 70% of cells that actively expressed *Thbs1* mRNA. Lack of TSP1 in Mφs decreased solution-based gelatinase activities by elevating tissue inhibitor of metalloproteinases-1 (TIMP1) without affecting the major matrix metalloproteinases (MMPs). Knocking down *Timp1* restored the ability of *Thbs1*^{−/−} Mφs to invade matrix. Finally, we generated *Thbs1*[flox/flox] mice and crossed them with *Lyz2-cre* mice. In the $CaCl_2$-induced model of AAA, lacking TSP1 in myeloid cells was sufficient to protect mice from aneurysm by reducing Mφ accumulation and preserving aortic integrity.

CONCLUSIONS: TSP1 contributes to aneurysm pathogenesis, at least in part, by suppressing TIMP1 expression, which subsequently enables inflammatory Mφs to infiltrate vascular tissues.
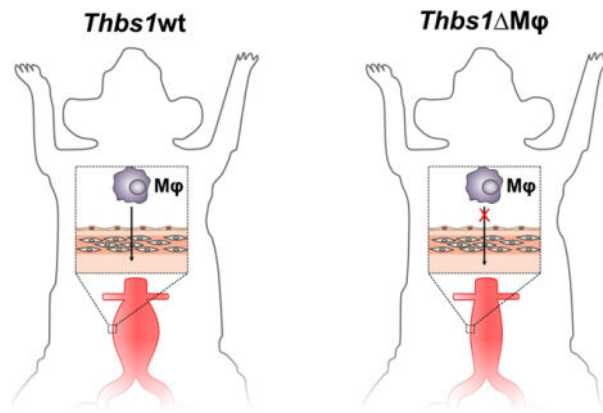
GRAPHICAL ABSTRACT:

[#]**Correspondence to:** Bo Liu, Ph. D., University of Wisconsin-Madison, 1111 Highland Avenue, WIMR 5137, Madison, WI 53705, Tel: 608-263-5931, Fax: 608-262-3330, liub@surgery.wisc.edu.
[*]These authors contributed equally.

Thbs1wt   *Thbs1ΔMφ*

Keywords

Thrombospondin-1; Abdominal aortic aneurysm; Macrophages; Inflammation; Tissue inhibitor of metalloproteinases-1

Subject codes

Aneurysm; Pathophysiology

Introduction

Aortic aneurysm is a focal dilatation of the aorta associated with substantial morbidity and mortality as a result of complications such as aortic rupture[1]. Although major progresses are achieved in diagnosis and surgical --- both open and endovascular --- aneurysm repair surgery, curative pharmacological treatments for this condition are still lacking[2, 3], highlighting a need to expand our knowledge of the mechanisms involved in development and progression of aortic aneurysm. Detailed pathological and imaging studies of human abdominal aortic aneurysm (AAA) revealed several major pathological features including extracellular matrix (ECM) degradation, loss of vascular smooth muscle cells (SMCs), and adventitial and medial inflammatory cell infiltration[4, 5]. Innate and adaptive immune cells, including neutrophils, macrophages (Mφs), dendritic cells, B cells, and T cells, have been identified in aortic aneurysms and are believed to contribute to aortic aneurysm development[1, 6]. Mφs are the most abundant immune cells found in the aneurysmal aortic wall of AAA[7] as well as animal models of AAA[8]. Accumulating experimental evidence demonstrates that Mφs contribute to the destruction of ECM and death or dysfunction of vascular SMCs by releasing a range of proteolytic enzymes (such as matrix metalloproteinases (MMPs) and cysteine proteases), -oxidation-derived free radicals and cytokines.[9–11].

Thrombospondin-1 (TSP1) is a member of the matricellular thrombospondin family. Through its modules or domains, TSP1 binds to various matrix proteins, integrins, and cell surface receptors including CD36 and CD47[12]. TSP1 is present at low levels in the wall of healthy blood vessels, and its vascular expression is upregulated in animal models of

atherosclerosis and ischemia-reperfusion injury[13, 14]. How levels of aortic TSP1 may be altered in aortic aneurysm is not clear. Our group found that levels of TSP1 are elevated in human and mouse AAA tissues[15]. Upregulated aortic TSP1 was also observed in human and experimental thoracic aortic aneurysm (TAA) by Yamashiro et al[16]. However, Krishna and colleagues reported reduced aortic TSP1 in aneurysm tissues[17]. Similarly, opposing outcomes were observed when deleting *Thbs1* ----- the gene encodes TSP1----- in mouse models for AAA and TAA[15–17]. These controversial findings may reflect the complexity of aneurysm pathophysiology and the multi-functionality of TSP1. Indeed, TSP1 can be both pro- and anti-inflammatory, depending on the cell types, cellular contents, and ECM environment which is unique to the nature and stage of any given disease[18–20]. For example, Moura et al demonstrated that *Thbs1* deficiency accelerates atherosclerotic plaque maturation and inflammation in the $Apoe^{-/-}$ background[14]. Using a diet-induced mouse model of obesity, Li et al reported that lacking TSP1, either globally or in myeloid cells, reduces obesity-associated inflammation or improves insulin sensitivity[21, 22]. $Thbs1^{-/-}$ mice also showed diminished Mφ recruitment into an excisional skin wound[23].

Since multiple cell types within the normal and aneurysmal aortic tissues are capable of producing TSP1, we postulate that TSP1 expression could be modulated by the disease process in a cell-specific manner. Here, we utilize conditional knockout approach to demonstrate that myeloid specific *Thbs1* deficiency protected mice from $CaCl_2$ induced AAA formation. RNA fluorescent *in situ* hybridization (RNA-FISH) further establishes Mφ being the major source of TSP1 elevation during AAA formation. *In vitro*, 3D migration assay showed deletion of *Thbs1* compromises matrigel invasion, which was resulted from a decline in solution-based gelatinase activity secondary to an up-regulation of tissue inhibitors of metalloproteinases-1 (TIMP1). This study highlights the importance of TSP1 in regulating Mφ function and its contribution to the complications in AAA pathogenesis *in vivo* and *in vitro*.

Material and methods

The data that support the findings of this study are available from the corresponding author upon reasonable request.

Reagents

Dulbecco's Modified Eagle's Medium (DMEM) and cell culture reagents were purchased from ThermoFisher Scientific. Mouse macrophage colony stimulating factor (M-CSF) was purchased from eBioscience (Cat. #14–8983–80). LPS was purchased from Sigma-Aldrich (Cat. # L4391). Recombinant mouse TNFα and IL4 were purchased from R&D Systems (Cat. # 410-MT and 404-ML, respectively). Elastic Stain kit was purchased from Sigma-Aldrich (Cat. # HT25A-1KT).

Human AAA samples

We obtained de-identified human AAA tissues that were removed as part of routine surgical AAA repair. The use of human tissues that would be otherwise discarded as surgical wastes

were under an exemption approved by the institutional ethics committee of University of Wisconsin – Madison.

Animal studies

All animal studies conformed to the National Institutes of Health (NIH) Guide for the Care and Use of Laboratory Animals and were performed with the approval of the Institute Animal Care and Use Committee at University of Wisconsin-Madison (Protocol # M005792). All experiments were performed on male mice, as AAAs predominantly affect men[24]. All mice had free access to standard laboratory diet (2018 Teklad global 18% protein rodent diets, ENVIGO) and water. *Thbs1*^{−/−} mice[25](Stock # 006141), C57BL/6J mice (*Thbs1*^{+/+}, Stock # 000664) and *Apoe*^{−/−} mice (Stock # 002052) were purchased from The Jackson Laboratory and maintained on homozygous breeding.

Generation of myeloid-specific *Thbs1* knockout mice

Thbs1 floxed mice were generated by inserting 2 loxP sites downstream of exon 3 and exon 7 of the *Thbs1* gene respectively. An FRT site flanked neomycin positive selection cassette was also included right before the 3'-loxP site. Thymidine kinase was used as a negative selection gene for the purpose of getting rid of cells with nonspecific integration. After homologous recombination in SV129-derived ES cells, removing of neomycin cassette, and injection of recombinant cells into C57BL/6 blastocysts, heterozygous floxed mice were mated to generate *Thbs1*[flox/flox] mice. *Thbs1*[flox/flox] mice were backcrossed to the C57BL/6 background for over 10 generations. Myeloid-specific *Thbs1* knockout mice were generated by breeding *Thbs1*[flox/flox] mice with *Lyz2-cre* mice[26] (The Jackson Laboratory, Stock # 004781). Experiments were performed using age matched *Thbs1*[wt/wt]*Lyz2-cre* and *Thbs1*[flox/flox]*Lyz2-cre* littermates.

Modified CaCl$_2$ model:

12–16-week-old male mice were anesthetized by isoflurane inhalation. Abdominal aorta was isolated following a midline incision. A small piece of gauze soaked in 0.5 M CaCl$_2$ was applied perivascularly for 10 minutes. The gauze was replaced with another piece of PBS-soaked gauze for 5 minutes. Mice in sham group received 0.5 M NaCl treatment for 10 minutes followed by PBS soaked gauze for 5 minutes. At selective time points, mice were euthanized and perfused, aortae were harvested and embedded with optimal cutting temperature compound (Sakura Tissue Tek). 6 μm cross sections were cut using Leica CM3050 S cryostat. The maximum external diameter of the infrarenal aorta was measured using a digital caliper prior to CaCl$_2$ or NaCl treatment (initial measurement) and at the time of tissue harvest (final measurement). Aortic dilation (% increase) relative to pre-treatment diameter was determined as: ((Final measurement – initial measurement)/Initial measurement) *100. An aneurysm was defined as a 50% increase in aortic diameter[15].

Angiotensin II model:

12–16-week-old male *Apoe*^{−/−} mice were anesthetized by isoflurane inhalation. Alzet osmotic minipumps (Model 2004, DURECT Corporation) were placed into the subcutaneous space of mice through a small incision in the back of neck. Incision was

closed and 2% lidocaine topical ointment was applied to the suture site. Pumps were filled either with PBS vehicle or solutions of Angiotensin II (A9525, Sigma-Aldrich) that delivered 1000 ng/kg/min of Angiotensin II[8].

Preparation of Bone Marrow-derived Macrophages

Bone marrow cells were collected from femurs and tibias of mice and differentiated into Bone Marrow Derived Macrophages (BMDM) using macrophage medium (DMEM with 10% FBS, 1% penicillin/streptomycin antibiotic, and 20 ng/ml mouse M-CSF). Medium was changed after three days of incubation at 37°C, 5% CO2. After a further four days culture, the adherent cells were harvested for experiments[15].

RNA Fluorescent *in situ* hybridization (RNA-FISH)

Paraffin-embedded human AAA tissue or fresh frozen murine aortic sections were examined using Advanced Cell Diagnostics (ACD) RNAscope® Fluorescent Multiplex Reagent Kit (320850) with RNAscope® Probe against human *THBS1* (320850), human *CD68* (560591-C3), mouse *Thbs1* (457891-C3), mouse *Cd68* (316611-C2), mouse *Pecam1* (316721). Probe against *DapB* (*dihydrodipicolinate reductase*, from Bacillus subtilis) was used as negative control (310043-C3), probe against *Ubc* (*Mus musculus ubiquitin C*) was used as positive control (310771-C3). Tissue pretreatment, probe hybridization and signal amplification were performed according to manufacturer's instructions. For RNA-FISH combined with immunostaining, after signal amplification, tissue sections were blocked with 10% normal donkey serum. Alexa Fluor® 488 anti-mouse MHC II antibody (1:100, 107616, clone M5/114.15.2, BioLegend) were applied onto tissue sections, and incubated 2 hours at room temperature. Images were acquired with a Nikon A1RS confocal microscope system and analyzed using ImageJ software.

Immunofluorescent staining

PFA-fixed tissue sections or cells were blocked with 10% normal donkey serum and incubated at 4 °C overnight with primary antibodies anti- TIMP1 (1:100, AF980, R&D Systems), anti- MYH11 (1:200, ab53219, Abcam), PE anti-mouse F4/80 (1:100, 123110, clone BM8, BioLegend). Normal goat or rabbit IgG was used as negative controls. After several washes with PBS, sections were incubated with Alexa Fluor 488- or Alexa Fluor 594-conjugated secondary antibodies for 1 hour at room temperature. DAPI was used to stain nuclei. Images were acquired with a Nikon A1RS confocal microscope system and analyzed using ImageJ software.

Single cell RNA sequencing analysis

Single cell RNA sequencing data were downloaded from https://www.ncbi.nlm.nih.gov/geo/query/acc.cgi?acc=GSE97310. Standard procedures for filtering, variable gene selection, dimensionality reduction, clustering, and gene expression visualization were performed using the Scanpy (29409532) Python package version 1.4.4 (https://github.com/theislab/scanpy). The Jupyter notebook containing Python script for the data processing were uploaded to https://github.com/iamyanghuan/TSP1/blob/master/Cochain18CircR.ipynb.

Processed data were uploaded to https://github.com/iamyanghuan/TSP1/blob/master/Conchain18CircR.h5ad.

Western blotting

Conditioned medium was concentrated using Amicon® Ultra-4 Centrifugal Filter Units (UFC801096, Millipore), cells were lysed in RIPA buffer (R0278, Sigma-Aldrich) containing protease and phosphatase inhibitors (Halt Cocktail, Thermo Scientific).

Concentrated medium or protein extract were loaded and separated by SDS-PAGE and then transferred to polyvinylidene fluoride membranes. The membranes were blocked with 5% skim milk, and incubated overnight at 4°C with the following primary antibodies: anti-MMP9 (1:1000, AF909, R&D Systems), anti-TIMP1 (1:1000, AF980, R&D Systems), anti-ACTB (1:5000, A5441, Sigma-Aldrich), followed by HRP-labeled secondary antibody (1:5000, Jackson ImmunoResearch).

RNA Isolation and Real-Time PCR (RT-PCR)

Total RNA was extracted from cultured cells using Trizol reagent (15596018, ThermoFisher Scientific) according to manufacturer's protocols. 1 μg total RNA was used for the first-strand cDNA synthesis followed by RT-PCR. Primer sequences used were: *Mmp2*: forward 5'-CTGGGAGCATGGAGATGGATAC-3', reverse 5'-TGGTAAACAAGGCTTCATGGGG-3'; *Mmp3*: forward 5'-TCTCCTTTGCAGTTGGAGAACA-3', reverse 5'-GAGAGATGGAAACGGGACAAGT-3'; *Mmp9*: forward 5'-AAAGGCAGCGTTAGCCAGAA-3', reverse 5'-TAGCGGTACAAGTATGCCTCTG-3'; *Mmp12*: forward 5'- AAAGTGGGGCTTTAAGGGAACT-3', reverse 5'-GACAAGTACCATTCAGCAAATTCAC-3'; *Mmp10*: forward 5'-ACTGGAGATTTGATGAGACAAGACA-3', reverse 5'-AACTGTGATGATCCTCGGAAGAAA-3'; *Il1b*: forward 5'-AAATGCCACCTTTTGACAGTGATG-3', reverse 5'-AGATTTGAAGCTGGATGCTCTCAT-3'; *Il6*: forward 5'-CCACCAAGAACGATAGTCAATTCC-3', reverse 5'-GCCATTGCACAACTCTTTTCTCA-3'; *Ccl2*: forward 5'-ATTCACCAGCAAGATGATCCCAAT-3', reverse 5'-TGAGCTTGGTGACAAAAACTACAG-3'; *Thbs1*: forward 5'-ACCGGTTATATCAGAGTGGTGATG-3', reverse 5'-TGTCTGAGAAGAACACCATTTCCT-3'; *Timp1*: forward 5'-GAAGCCTGGAGGCAGTGATT-3', reverse 5'-GTACGCCAGGGAACCAAGAA-3'; *Timp2*: forward 5'- CTCCCCTGTCTCTACACACACC-3', reverse 5'-GAGGGGGAGTCCTTAACCGT-3'; *Timp3*: forward 5'-AGTGGGTCTCACAGTTATCCA-3', reverse 5'-GCTGAACCCAGGCAGATGTT-3'; *Timp4*: forward 5'- TGGCTGCCAATGCCATGTA-3', reverse 5'-TATCTGGCAGCAACACAGCA-3'; *Arg1*: forward 5'-GCTTCGGAACTCAACGGGA-3', reverse 5'-CTTAGTTCTGTCTGCTTTGCTG-3'; and *Actb*: forward 5'-AGCCTTCCTTCTTGGGTATGG-3', reverse 5'-AAGGGTGTAAAACGCAGCTCA-3'.

siRNA-mediated knock-down

BMDM were transfected with scrambled siRNA and siRNA against mouse *Timp1* by using Opti-MEM (51985034, Gibco) and Lipofectamine RNAiMAX (13778150, Invitrogen) for 48 hours. SiRNAs were purchased from Integrated DNA Technologies, design ID: mm.Ri.Timp1.13.

3D inverted Matrigel infiltration assay

100 μl of Matrigel (BD Biosciences; stock mixed 1:1 with ice-cold PBS and supplemented with bovine plasma fibronectin to a final concentration of 50 μg/mL), was transferred to a transwell insert (8 μm pore, Corning) to polymerise at 37 °C, 5% CO_2. After polymerisation, Transwell inserts were inverted and 5×10^4 BMDMs were applied directly to the underside of the insert filter and allowed to adhere for 2 h. Non-adherent cells were removed, and transwell inserts were placed into a chamber containing macrophage medium with PBS or 100 ng/mL LPS was applied to the upper transwell chamber to establish a chemotactic gradient through the Matrigel/fibronectin gel.

Transwell cultures were incubated for 5 days to allow invasion into the gel. Cells were then stained with 10 μg/ml Hoechst 33342 (H3570, Invitrogen). Confocal images of cells adherent to the filter were obtained, to confirm cell adhesion had remained constant across conditions during the experiment. These cells were then removed with a cotton swab to ensure only migrating cells were analyzed. Serial confocal optical sections (20 μm) of the Matrigel/fibronectin gel were captured with a Nikon A1RS confocal microscope system. Confocal data was collected from 5 fields of view per transwell and quantified using ImageJ software[27].

In rescue assay, BMDMs were prelabeled with CellTracker Blue CMAC Dye (C2110, Invitrogen), and mixed with equal number of unlabeled BMDMs. Cell mixture were seeded onto the underside of the Transwell inserts as mentioned above. After 5 days, cells migrated into the Matrigel/fibronectin gel were examined by confocal microscopy without additional staining.

Gel zymography

Conditioned medium from BMDMs were concentrated by passing through Amicon® Ultra-4 Centrifugal Filter Units (Cat. # UFC801096, Millipore) at 4000 rpm for 30min at 4°C. Concentrated conditioned medium were then mixed with 5X non-reducing sample buffer and loaded in Novex 10% Zymogram Plus (Gelatin) gel (ZY00100BOX, Invitrogen) run at 150 V until good band separation was achieved. Novex™ Zymogram Renaturing Buffer (LC2670, Invitrogen), Zymogram Developing Buffer (LC2671, Invitrogen) and SimplyBlue™ SafeStain (LC6060, Invitrogen) were incubated with the gel in sequence according to the manufacturer's instructions to visualize bands.

Solution-based gelatinase activity assay

Fresh prepared concentrated conditioned medium was subjected to the EnzChek® Gelatinase/Collagenase Assay Kit (E-12055, Invitrogen) according to the product's manual.

***In situ* zymography**—*In situ* zymography was described previously[28]. Briefly, 1mg/ml Fluorescein Conjugated DQ™ Gelatin From Pig Skin (D12054, Invitrogen) was diluted 20 times with 70 °C melted 1% UltraPure™ Low Melting Point Agarose (16520100, Invitrogen) in PBS and immediately applied to the fresh frozen sections followed by quick coverslip mounting. After the agarose set, the samples were then incubated at 37 °C for 2 hours and immediately subjected to confocal microscopy. During the capturing, unimaged specimens were stored on ice to slow down the enzyme reaction.

Statistical analysis

Results are presented as mean ± SD. Data were assessed for normality using Shapiro-Wilk normality test. Data not exhibiting a normal distribution were log2-transformed and retested for normality. Two-tailed Student's t test for normally distributed data and Mann–Whitney nonparametric test for skewed data that remained deviate from normality after transformation were used to compare between two conditions. One-way Analysis of Variance (ANOVA) with Tukey post hoc test for normally distributed data and Kruskal–Wallis nonparametric test for skewed data after transformation were used to compare   three means. Two-way ANOVA followed by Sidak multiple comparisons were performed to compare how a response is affected by two factors. Statistical analyses were performed with GraphPad Prism 7.0 (GraphPad Software, Inc.). Experiments were repeated as indicated. Differences with $p<0.05$ were considered statistically significant.

Results

Mφs are the major cell type responsible for elevated *Thbs1* expression in AAA

RNA-FISH analysis showed that normal aortic walls of adult mice expressed low level of *Thbs1* mRNA, primarily in endothelial cells (Supplemental Figure I). The specificity of the probe against *Thbs1* was validated using aortic tissue from *Thbs1*^{−/−} mice (Supplemental Figure I). Aneurysm induced by $CaCl_2$ or Angiotensin II increased biosynthesis of *Thbs1* mRNA (Figure 1A&C), which is consistent with our prior report[15]. In the challenged aorta, *Thbs1*-expressing cells predominantly located in adventitia. There was a significant co-localization between *Thbs1* and *Cd68* mRNA. In both murine models of AAA, over 70% of *Thbs1*-expressing cells co-expressed *Cd68* mRNAs (Figure 1B&D). Similarly, the majority of the *Thbs1*-expressing cells also expressed *CD68* in human aneurysmal tissues (Figure 1E). These data, along with our previously published co-immunostaining data[15], indicate that Mφs are the major source of TSP1 in aneurysm tissues.

Thbs1-expressing Mφs are pro-inflammatory

To characterize *Thbs1*-expressing Mφs, we analyzed $CaCl_2$-treated mouse aortic tissues using RNA-FISH combined with immunofluorescent staining. As shown in Figure 2A, 68% *Cd68* positive cells expressed *Thbs1*. Among these *Thbs*1-expressing Mφs, 66% of them were stained positively for class II major histocompatibility complex (MHC II), a marker of activated Mφs[9]. We further tested whether *Thbs1* expression in Mφs are associated with inflammatory states by analyzing published single cell RNA sequencing data of immune cells (*Cd45+*) in mouse atherosclerotic plaques (GSE97310)[29]. Among the 13 plaque-associated cell clusters, 6 clusters are Mφs identified by high expression of *Cd68*, *Csf1r*, and

Adegre1. Thbs1 expression was highest in Mφ cluster 3 & 10, which also contained high levels of well-known pro-inflammatory cytokines including *Il1b, Socs3*, and *Tnf* as well as high levels of Mφ activation markers such as *H2-Ab1* and *Cd86* (Figure 2B&C). In contrast, Mφs containing high levels of anti-inflammatory cytokines, and dendritic, B, T, NK cells produced low level of *Thbs1* mRNAs (Figure 2C). Consistently, we found that bone marrow derived Mφs (BMDM) from wildtype mice responded to TNFα and LPS with increased expression of *Thbs1* mRNA, while IL4 stimulation didn't affect *Thbs1* mRNA level (Figure 2D).

TSP1 is necessary for effective Mφ infiltration into ECM

We have previously shown *Thbs1⁻/⁻* mice responded to aneurysm induction with significantly reduced aortic infiltration of monocytes and Mφs[15]. However, lacking TSP1 did not change blood cell composition. Cell counts for monocytes, neutrophils, lymphocytes and total white blood cells were similar between whole blood from *Thbs1⁺/⁺* and *Thbs1⁻/⁻* mice (Supplemental Figure IIA). In addition, deficiency of *Thbs1* did not affect *in vitro* differentiation of bone marrow cells into Mφs (Supplemental Figure IIB). Furthermore, devoid of *Thbs1* in BMDMs did not alter the expression of pro-inflammatory cytokine or chemokine (*Il1b, Il6* and *Ccl2*) or anti- inflammatory enzyme *Arg1* (Supplemental Figure IIC–F). Next, we examined Mφ migration using a 3D inverted infiltration system in which BMDMs were allowed to migrate through a matrix containing 50% Matrigel and 50 μg/ml fibronectin toward a chemokine gradient (Figure 3A). Compared to wildtype Mφs, *Thbs1⁻/⁻* Mφs showed remarkably decreased ability to invade the matrix particularly in the depth beyond 20 μm (Figure 3B&C). Of note, premixing *Thbs1⁻/⁻* Mφs with *Thbs1⁺/⁺* Mφs did not rescue the invasion defects (Figure 3D&E), recombinant TSP1 also showed very low permeability through Matrigel (Supplemental Figure III). These results indicate that TSP1 is required for effective infiltration into ECM through an autocrine mechanism.

Lack of *Thbs1* causes reduction of MMP activity in Mφs

Mφs require MMPs for persistent and directional migration into ECM[9]. We thus measured gelatinase activity in conditioned medium from *Thbs1⁺/⁺* and *Thbs1⁻/⁻* BMDMs. In solution-based fluorometric assay, *Thbs1⁻/⁻* BMDMs produced significantly less gelatinase activity than the wildtype Mφs at the baseline. This reduction became more profound when stimulated with LPS, because LPS greatly enhanced gelatinase activities of wildtype Mφs, but not mutant Mφs (Figure 4A). However, gel zymography and Western blotting showed that *Thbs1* knockout did not decrease MMP9 activity or protein levels (Figure 4B–E). RT-PCR analysis confirmed that lacking TSP1 did not reduce levels of *Mmp9* as well as other MMPs known to be produced by BMDMs[27] including *Mmp3, Mmp10* and *Mmp12* (Figure 4F–I). We were unable to determine the effects on *Mmp2, Mmp8* and *Mmp13* due to the low expression levels (data not shown). Taken together, lack of TSP1 suppressed extracellular gelatinase activity in solution-based assay without reducing MMP activities or expression levels.

TIMP1 is upregulated in *Thbs1* deficient BMDMs

We speculated that the diminished solution-based gelatinase activity in *Thbs1⁻/⁻* BMDMs resulted from upregulated TIMPs, the endogenous inhibitors against MMPs[30]. Four TIMP

isoforms are expressed by Mφs[27]. By Real-Time PCR, we noted that *Timp1* mRNA increased ~70% in *Thbs1*^{−/−} BMDMs as compared to *Thbs1*^{+/+} cells upon LPS stimulation, while *Timp2* or *Timp3* were not significantly altered (Figure 5A–C). *Timp4* was undetectable in BMDMs under conditions we used (data not shown). Immunofluorescent staining and Western blotting confirmed the upregulation of TIMP1 in *Thbs1*^{−/−} BMDMs (Figure 5D–F). To prove whether TIMP1 is responsible for the reduction of solution-based gelatinase activity, we used 3 siRNAs targeting different regions of the *Timp1* mRNA. Compared to the scramble control, siRNA No.2 and 3 showed ~60% RNA interference (RNAi) efficiency, while siRNA No. 1 had minimum RNAi activity (Figure 5G). We then tested gelatinase activity in conditioned medium from *Thbs1*^{−/−} BMDMs transfected with *Timp1* siRNAs for 48 hours followed by LPS stimulation. SiRNA No.2 and 3 but not No. 1 successfully restored gelatinase activity of *Thbs1*^{−/−} BMDMs in solution-based fluorometric assay (Figure 5H). Moreover, migration of *Thbs1*^{−/−} BMDMs was also rescued by effective RNAi (Figure 5I). Collectively, these data demonstrate that elevated TIMP1 is the primary cause of proteolytic and migratory defects of *Thbs1* knockout Mφs.

Thbs1 deficient aorta displays higher TIMP1 levels than the wildtype control.

Next, we examined aortic expression of TIMP1 in aneurysm. Both Mφs (F4/80 positive) and SMCs (MYH11 positive) expressed TIMP1 in aneurysmal aorta (Supplemental Figure IV). On Day 4 after CaCl2 challenge, a time point when inflammation is prominent, TIMP1 was dramatically up-regulated in *Thbs1*^{−/−} aortic wall, in both adventitia and tunica media (Figure 5J&K). To address whether gelatinase activity is affected, we performed *in situ* zymography on freshly frozen aneurysmal tissues. *Thbs1* knockout reduced gelatinase activity by ~50%, which was inversely correlated to the TIMP1 upregulation (Figure 5L&M).

Myeloid-specific *Thbs1* deficiency attenuates AAA

Having identified Mφ-TSP1 being a major component responsible for the inflammatory and proteolytic responses during aneurysm development, we sought to delete *Thbs1* in Mφs. We generated *Thbs1*[flox/flox] mice, then crossed with *Lyz2-cre* mice to generate myeloid-specific *Thbs1* knockout mice as outlined in Supplemental Figure VA. Efficiency and specificity of conditional knockout mice were evaluated by *in situ* hybridization. In naïve aorta, both *Thbs1*[wt/wt]/*Lyz2-cre* mice (*Thbs1*wt) and *Thbs1*[flox/flox]/*Lyz2-cre* mice (*Thbs1* Mφ) expressed *Thbs1* in endothelial cells (*Pecam1* positive cells) (Supplemental Figure VB). To detect *Thbs1* expression in myeloid cells, we subjected mice to CaCl2 induced AAA model. Four days after CaCl2 application, *Thbs1*wt showed high expression of *Thbs1* in *Cd68* positive Mφs, while Mφs of *Thbs1* Mφ didn't express *Thbs1* (Supplemental Figure VC). To determine how conditional loss of TSP1 affects aneurysm formation, we measured external aortic diameter 28 days after AAA induction. Compared to *Thbs1*wt, *Thbs1* Mφ showed much reduced aneurysmal sizes. Specifically, only 1 of 5 *Thbs1* Mφ developed aneurysm as compared to 5 out of 6 aneurysm incidence in *Thbs1*wt. The aortic dilation was greatly reduced in *Thbs1* Mφ (percentage increase of external diameter relative to pre-aneurysm induction *Thbs1*wt: 70.24±21.68% vs *Thbs1* Mφ: 38.66±13.08%; $p<0.05$) (Figure 6A&B). SMC phenotypic change is another major underlying mechanism of AAA characterized by loss of contractile protein such as myosin heavy chain 11 (MYH11) and gain of synthetic

markers such as vimentin. The conditional knockout did not significantly affect SMC phenotypes judging by the similar medial levels of MYH11 and vimentin in *Thbs1* Mφ mice and their wildtype counterparts (Figure 6C&D and Supplemental Figure VI). Additionally, *Thbs1* Mφ mice showed an amelioration of breakage of elastin demonstrated by elastic staining (Figure 6E).

Myeloid-specific *Thbs1* deficiency reduces Mφ accumulation

To assess whether myeloid-specific *Thbs1* deficiency influences Mφ infiltration *in vivo*, we stained the aortic tissues with Mφ marker F4/80. The aortic accumulation of Mφs was significantly reduced in the conditional knockout group (Figure 6F&G). Consistent with total body *Thbs1* knockout mice, upregulation of TIMP1 and decline of gelatinase activity were also observed in the *Thbs1* Mφ aneurysmal aortic wall (Figure 6H–K).

Discussion

ECM degradation and Mφ infiltration are key features of AAA pathology[31]. Here, we report that inflammatory Mφs are the major source of TSP1 accumulation in AAA. Elevated TSP1 empowers Mφ mobility by suppressing *Timp1* expression, which subsequently enables MMPs activation, ECM degradation and tissue infiltration (Figure 7). These results provide new mechanistic insights on vascular inflammation during AAA development.

Consistent with their role in wound healing, the thrombospondin family of matricellular proteins including TSP1, TSP2, and TSP4 are frequently upregulated following tissue injury[32]. However, mixed findings have been reported regarding how levels of TSP1 changes in aortic aneurysm. Our prior study showed that levels of TSP1 are elevated in human and mouse AAA tissues comparing to non-aneurysm tissues[15]. Upregulated aortic TSP1 was also observed in human and experimental thoracic aortic aneurysm (TAA) by Yamashiro et al[16]. However, Krishna and colleagues reported reduced aortic TSP1 in aneurysm tissues relative to proximal macroscopically non-dilated abdominal aortic tissue[17]. In animal studies, we induced AAA by intravascularly perfusion of elastase or perivascularly application of $CaCl_2$ followed by PBS. In both models, $Thbs1^{-/-}$ mice showed aneurysm-resistant phenotype. Golledge et al.[17] crossed $Thbs1^{-/-}$ mice with $Apoe^{-/-}$ mice and infused mice with Angiotensin II. They found $Thbs1^{-/-} Apoe^{-/-}$ mice augmented AAA growth compared to $Apoe^{-/-}$ mice. It is possible that the different outcomes of *Thbs1* deletion is caused by different mouse models used between different groups. We also speculate that that TSP1 may have both pro- and anti-inflammatory functions in aneurysmal disease, depending on the cell types, cellular contents, and ECM environment that is likely to be differentially altered in different aneurysm models.

In this study, our *in situ* hybridization results demonstrated that *Thbs1* mRNA expression was elevated in two mouse models of AAA, which was consistent with our previous findings using RT-PCR and immunohistochemistry[15]. Furthermore, the *in situ* hybridization approach revealed the special expression pattern of *Thbs1* expression: the adventitial Mφs being the major cell type that were actively expressing *Thbs1* mRNA in the mouse aneurysmal aorta. Due to the unavailability of age matched healthy aortic tissues, we were unable to access whether levels of *Thbs1* mRNA were also elevated in human aneurysmal tissues. However,

human aneurysmal tissues we analyzed contained abundant *Thbs1* mRNA, which was predominantly colocalized to Mφs.

Our *in situ* and immunohistological analyses showed that Mφs containing high levels of *Thbs1* transcripts were positive of various inflammatory markers. The notion that inflammatory Mφs being the major source of TSP1 in disease is supported by the single cell RNA sequencing data from atherosclerotic plaques. Together, these data suggest that elevated expression of *Thbs1* is part of the transcriptome profile of inflammatory Mφs. However, TSP1 itself might not be required by Mφs to undergo M1-like polarization because *Thbs1* null Mφs showed similar *in vitro* response to LPS as wildtype Mφs. It is important to note the M1 versus M2 polarization is largely an *in vitro* concept which does not represent the complex biology of Mφs in diseases. While additional studies are needed to evaluate Mφ phenotypes during aneurysm development, mixed reports were found in the literature about whether TSP1 promotes inflammatory or anti-inflammatory differentiation of Mφs. TSP1 facilitates activation of inflammatory Mφs through TLR4 signaling[33], whereas Zhao and Stein et al reported that TSP1 stimulates Mφ IL-10 expression in experimental lung injury[34] and limits IL-1β expression[35].

We postulate that TSP1 regulates Mφ migration through an autocrine mechanism because adding *Thbs1*$^{+/+}$ Mφs did not rescue the migratory defect of *Thbs1*$^{-/-}$ Mφs in the *in vitro* Matrigel infiltration assay. It is unclear why the wildtype cells failed to rescue the mutant cells since TSP1 is a secreted protein. However, we found that recombinant TSP1 protein had very low permeability through Matrigel. The low diffusion rate, along with its ability to bind to many proteins in the matrix, may explain why TSP1 secreted by one cell may not be readily available to other cells.

Evidence obtained in the current study suggests that TSP1 plays an important role in regulation of aortic accumulation of monocyte/Mφs during the development of AAA. *Thbs1* gene deficiency in myeloid lineage was sufficient to attenuate AAA formation at least in the CaCl$_2$ model. The myeloid-specific *Thbs1* knockout mice had much diminished Mφ accumulation and gelatinase activity in aneurysmal aorta. The aneurysm- and inflammation-resistant phenotype of the conditional knockouts resembled that of *Thbs1* global knockout mice[15]. The phenotypic similarities between the two strains of TSP1 mutant mice suggest that TSP1 contributes to aneurysm pathogenesis largely through myeloid cells. Based on the results of *in situ* hybridization analysis, we postulate TSP1 expressed by inflammatory Mφs is the major culprit, however, this notion remains to be tested when a Mφ-specific Cre becomes available. It is worth of noting that Memetimin et al reported a similar connection between TSP1 and Mφ -mediated inflammation[21]. The authors generated a different strain of *Thbs1* floxed mice and crossed them to *Lyz2-Cre*. In a long-term diet-induced obesity model, myeloid-specific loss of TSP1 reduces Mφ accumulation in adipose tissues, which phenocopies the global *Thbs1* knockouts reported by the same group earlier[22]. However, the role of TSP1 in Mφ accumulation is likely to be complex because enhanced inflammation by global *Thbs1* knockout was found in experimental models of atherosclerosis[14], myocardial infarcts[36], exudative age-related macular degeneration[37], lung injury[34] and Angiotensin II induced aortic aneurysm[17].

Mechanistically, our *in vitro* data suggest the upregulated TIMP1 is responsible for the migratory defect of *Thbs1*$^{-/-}$ Mφs. TIMPs are endogenous inhibitors to MMPs and disintegrin-metalloproteinases (ADAMs and ADAMTSs)[38]. TIMP family includes TIMP1, TIMP2, TIMP3, and TIMP4. Consistent with the literature[39, 40], we found *Timp4* expression was not detectable in Mφs. Among *Timp1*, *Timp2*, and *Timp3*, only levels of *Timp1* were affected by *Thbs1* knockout. Most importantly, silencing *Timp1* using siRNA in *Thbs1*$^{-/-}$ Mφs restored solution-based gelatinase activity and infiltrating ability of the mutant cells. It is unclear how TSP1 suppresses TIMP1 expression in Mφs. Opposite regulation of TIMP1 by TSP1 was observed by John et al, in human breast and prostate cancer cell lines[41]. Based on the observation that *Thbs1*$^{-/-}$ choroidal endothelial cells showed increased phosphorylated endothelial nitric oxide synthase (eNOS) and inducible NOS (iNOS), as well as increased signal transducer and activator of transcription 3 (STAT3) phosphorylation[42], we speculate that TSP1 inhibits TIMP1 expression via CD47-eNOS-NO-TGFβ-Smad axis, or/and through activation of STAT3. This theory is supported by prior studies in which nitric oxide enhances IL-1β induced *Timp1* expression by activating TGFβ-Smad signaling in glomerular mesangial cells[43]. Additionally, phospho-STAT3 was found to bind to the *Timp1* promoter and activate *Timp1* expression in Huh7 cells[44]. However, whether TSP1 signals through the similar mechanisms in Mφs warrants further investigation.

The protective role of TIMP1 in AAA has been explored by several investigative groups. Expression of TIMP1 was found to be increased in both human and mouse AAA[45, 46], likely as part of compensatory mechanism. *Timp1*$^{-/-}$ mice develop significantly larger aneurysm in various AAA models[47–49]. Overexpressing *Timp1* prevents AAA progression[50]. In this study, both global *Thbs1* deficient mice and *Thbs1* Mφ showed elevated TIMP1 level, especially in medial SMC layer. *Thbs1* Mφ also had more preserved SMCs in aneurysmal aorta compared to wildtype control, suggesting that *Thbs1* deletion in Mφ might have an indirect role in regulating TIMP1 level in SMCs, and maintaining SMC phenotype.

It is somewhat unexpected that we found no significant reductions in MMP protein and mRNA levels in *Thbs1*$^{-/-}$ Mφs. TSP1 upregulates MMP9 in endothelial cells[51, 52], cancer cells such as human squamous cell carcinoma cells[53], pancreatic cancer cells[54], and gastric cancer[55]. Global knockout *Thbs1* in mice decreased MMP9 activity in the heart[56], inhibited the elevation of MMP9 activity in aortae of carotid artery ligation model[57] and in cornea after desiccating stress[58]. However, cellular and tissue MMP activities are determined by the balance between levels of MMPs and TIMPs. Using solution-based fluorometric assay, our results showed that conditioned medium from *Thbs1*$^{-/-}$ Mφs had lower gelatinase activity both at baseline and after LPS stimulation. However, MMP9 activity or expression levels were not affected by *Thbs1* deficiency. The absence of changes in mRNA levels of other MMPs such as *Mmp3*, *Mmp10* or *Mmp12* further suggests that the reduced gelatinase activity of *Thbs1*$^{-/-}$ Mφs in solution-based assay is not resulted from a direct regulation at the MMP expression or activation.

There are several limitations in this study. As mentioned earlier in the discussion, *Lyz2-cre* leads to deletion of *Thbs1* in monocyte/Mφs, granulocytes and few CD11c+ dendritic cells[59]. Neutrophil is critically important to aneurysm formation[60], however, how TSP1 may affect neutrophil function in the context of AAA is not clear. We also did not examine the

Author Manuscript

expression of all proteases in wildtype and *Thbs1*$^{-/-}$ BMDMs, including MMP-14. Another limitation is related to the animal model. Currently, there is no single animal model that reflects the full disease spectrum of human AAAs. In this study, we demonstrated that *Thbs1*⁻ Mφ inhibited AAA in murine CaCl$_2$ model. Further evaluation of *Thbs1*⁻ Mφ, as well as conditional knockout in other vascular cell types, in other AAA models will be informative. The current study is also limited by the lack of functional data from human primary Mφs.

In conclusion, we demonstrated that TSP1 was mainly expressed by Mφs in AAA, especially inflammatory Mφs. TSP1 enhanced Mφ infiltration both *in vitro* and *in vivo*, likely through inhibiting TIMP1 expression. Myeloid-specific knockout of *Thbs1* blocked aneurysm growth in CaCl$_2$ induced AAA, and inhibited vascular inflammation. Since Mφ is a critical component of tissue remodeling and inflammation, our findings provide scientific rationale to therapeutic development of anti-TSP1 strategies in aneurysm.

Supplementary Material

Refer to Web version on PubMed Central for supplementary material.

Acknowledgments

Non-standard Abbreviations and Acronyms

AAA	Abdominal aortic aneurysm
Mφ	Macrophage
TSP1	Thrombospondin-1
TIMP1	Tissue inhibitor of metalloproteinases-1
ECM	Extracellular matrix
SMC	Smooth muscle cell
MMP	Matrix metalloproteinase
RNA-FISH	RNA fluorescent *in situ* hybridization
BMDMs	Bone marrow derived macrophages

References

1. Golledge J Abdominal aortic aneurysm: Update on pathogenesis and medical treatments. Nat Rev Cardiol. 2019;16:225–242 [PubMed: 30443031]

2. Wang YD, Liu ZJ, Ren J, Xiang MX. Pharmacological therapy of abdominal aortic aneurysm: An update. Curr Vasc Pharmacol. 2018;16:114–124 [PubMed: 28412911]

3. Lindeman JH, Matsumura JS. Pharmacologic management of aneurysms. Circ Res. 2019;124:631–646 [PubMed: 30763216]

4. Daugherty A, Cassis LA. Mouse models of abdominal aortic aneurysms. Arterioscler Thromb Vasc Biol. 2004;24:429–434 [PubMed: 14739119]

5. Quintana RA, Taylor WR. Cellular mechanisms of aortic aneurysm formation. Circ Res. 2019;124:607–618 [PubMed: 30763207]

6. Dale MA, Ruhlman MK, Baxter BT. Inflammatory cell phenotypes in aaas: Their role and potential as targets for therapy. Arterioscler Thromb Vasc Biol. 2015;35:1746–1755 [PubMed: 26044582]

7. Satta J, Laurila A, Paakko P, Haukipuro K, Sormunen R, Parkkila S, Juvonen T. Chronic inflammation and elastin degradation in abdominal aortic aneurysm disease: An immunohistochemical and electron microscopic study. European journal of vascular and endovascular surgery : the official journal of the European Society for Vascular Surgery. 1998;15:313–319

8. Daugherty A, Manning MW, Cassis LA. Angiotensin ii promotes atherosclerotic lesions and aneurysms in apolipoprotein e-deficient mice. J Clin Invest. 2000;105:1605–1612 [PubMed: 10841519]

9. Raffort J, Lareyre F, Clement M, Hassen-Khodja R, Chinetti G, Mallat Z. Monocytes and macrophages in abdominal aortic aneurysm. Nat Rev Cardiol. 2017;14:457–471 [PubMed: 28406184]

10. Wang Q, Ren J, Morgan S, Liu Z, Dou C, Liu B. Monocyte chemoattractant protein-1 (mcp-1) regulates macrophage cytotoxicity in abdominal aortic aneurysm. PLoS One. 2014;9:e92053 [PubMed: 24632850]

11. Longo GM, Xiong W, Greiner TC, Zhao Y, Fiotti N, Baxter BT. Matrix metalloproteinases 2 and 9 work in concert to produce aortic aneurysms. J Clin Invest. 2002;110:625–632 [PubMed: 12208863]

12. Adams JC, Lawler J. The thrombospondins. Cold Spring Harbor Perspectives in Biology. 2011;3

13. Favier J, Germain S, Emmerich J, Corvol P, Gasc J-M. Critical overexpression of thrombospondin 1 in chronic leg ischaemia. The Journal of Pathology. 2005;207:358–366 [PubMed: 16110458]

14. Moura R, Tjwa M, Vandervoort P, Van Kerckhoven S, Holvoet P, Hoylaerts MF. Thrombospondin-1 deficiency accelerates atherosclerotic plaque maturation in apoe−/− mice. Circ Res. 2008;103:1181–1189 [PubMed: 18818405]

15. Liu Z, Morgan S, Ren J, Wang Q, Annis DS, Mosher DF, Zhang J, Sorenson CM, Sheibani N, Liu B. Thrombospondin-1 (tsp1) contributes to the development of vascular inflammation by regulating monocytic cell motility in mouse models of abdominal aortic aneurysm. Circ Res. 2015;117:129–141 [PubMed: 25940549]

16. Yamashiro Y, Thang BQ, Shin SJ, Lino CA, Nakamura T, Kim J, Sugiyama K, Tokunaga C, Sakamoto H, Osaka M, Davis EC, Wagenseil JE, Hiramatsu Y, Yanagisawa H. Role of thrombospondin-1 in mechanotransduction and development of thoracic aortic aneurysm in mouse and humans. Circ Res. 2018;123:660–672 [PubMed: 30355232]

17. Krishna SM, Seto SW, Jose R, Li J, Moxon J, Clancy P, Crossman DJ, Norman P, Emeto TI, Golledge J. High serum thrombospondin-1 concentration is associated with slower abdominal aortic aneurysm growth and deficiency of thrombospondin-1 promotes angiotensin ii induced aortic aneurysm in mice. Clin Sci (Lond). 2017;131:1261–1281 [PubMed: 28364044]

18. Rogers NM, Yao M, Novelli EM, Thomson AW, Roberts DD, Isenberg JS. Activated cd47 regulates multiple vascular and stress responses: Implications for acute kidney injury and its management. Am J Physiol Renal Physiol. 2012;303:F1117–1125 [PubMed: 22874763]

19. Rogers NM, Ghimire K, Calzada MJ, Isenberg JS. Matricellular protein thrombospondin-1 in pulmonary hypertension: Multiple pathways to disease. Cardiovasc Res. 2017;113:858–868 [PubMed: 28472457]

20. Murphy-Ullrich JE. Thrombospondin 1 and its diverse roles as a regulator of extracellular matrix in fibrotic disease. J Histochem Cytochem. 2019:22155419851103

21. Memetimin H, Li D, Tan K, Zhou C, Liang Y, Wu Y, Wang S. Myeloid-specific deletion of thrombospondin 1 protects against inflammation and insulin resistance in long-term diet-induced obese male mice. Am J Physiol Endocrinol Metab. 2018;315:E1194–E1203 [PubMed: 30351986]

22. Li Y, Tong X, Rumala C, Clemons K, Wang S. Thrombospondin1 deficiency reduces obesity-associated inflammation and improves insulin sensitivity in a diet-induced obese mouse model. PLoS One. 2011;6:e26656 [PubMed: 22039525]

23. Agah A, Kyriakides TR, Lawler J, Bornstein P. The lack of thrombospondin-1 (tsp1) dictates the course of wound healing in double-tsp1/tsp2-null mice. The American Journal of Pathology. 2002;161:831–839 [PubMed: 12213711]

24. Kent KC, Zwolak RM, Egorova NN, Riles TS, Manganaro A, Moskowitz AJ, Gelijns AC, Greco G. Analysis of risk factors for abdominal aortic aneurysm in a cohort of more than 3 million individuals. J Vasc Surg. 2010;52:539–548 [PubMed: 20630687]

25. Lawler J, Sunday M, Thibert V, Duquette M, George EL, Rayburn H, Hynes RO. Thrombospondin-1 is required for normal murine pulmonary homeostasis and its absence causes pneumonia. J Clin Invest. 1998;101:982–992 [PubMed: 9486968]

26. Clausen BE, Burkhardt C, Reith W, Renkawitz R, Forster I. Conditional gene targeting in macrophages and granulocytes using lysmcre mice. Transgenic Res. 1999;8:265–277 [PubMed: 10621974]

27. Murray MY, Birkland TP, Howe JD, Rowan AD, Fidock M, Parks WC, Gavrilovic J. Macrophage migration and invasion is regulated by mmp10 expression. PLoS One. 2013;8:e63555 [PubMed: 23691065]

28. Hadler-Olsen E, Kanapathippillai P, Berg E, Svineng G, Winberg JO, Uhlin-Hansen L. Gelatin in situ zymography on fixed, paraffin-embedded tissue: Zinc and ethanol fixation preserve enzyme activity. J Histochem Cytochem. 2010;58:29–39 [PubMed: 19755718]

29. Cochain C, Vafadarnejad E, Arampatzi P, Pelisek J, Winkels H, Ley K, Wolf D, Saliba AE, Zernecke A. Single-cell rna-seq reveals the transcriptional landscape and heterogeneity of aortic macrophages in murine atherosclerosis. Circ Res. 2018;122:1661–1674 [PubMed: 29545365]

30. Brew K Reflections on the evolution of the vertebrate tissue inhibitors of metalloproteinases. FASEB J. 2019;33:71–87 [PubMed: 30125136]

31. Trollope A, Moxon JV, Moran CS, Golledge J. Animal models of abdominal aortic aneurysm and their role in furthering management of human disease. Cardiovasc Pathol. 2011;20:114–123 [PubMed: 20133168]

32. Chistiakov DA, Melnichenko AA, Myasoedova VA, Grechko AV, Orekhov AN. Thrombospondins: A role in cardiovascular disease. Int J Mol Sci 2017;18

33. Li Y, Qi X, Tong X, Wang S. Thrombospondin 1 activates the macrophage toll-like receptor 4 pathway. Cell Mol Immunol. 2013;10:506–512 [PubMed: 23954950]

34. Zhao Y, Xiong Z, Lechner EJ, Klenotic PA, Hamburg BJ, Hulver M, Khare A, Oriss T, Mangalmurti N, Chan Y, Zhang Y, Ross MA, Stolz DB, Rosengart MR, Pilewski J, Ray P, Ray A, Silverstein RL, Lee JS. Thrombospondin-1 triggers macrophage il-10 production and promotes resolution of experimental lung injury. Mucosal Immunol. 2014;7:440–448 [PubMed: 24045574]

35. Stein EV, Miller TW, Ivins-O'Keefe K, Kaur S, Roberts DD. Secreted thrombospondin-1 regulates macrophage interleukin-1beta production and activation through cd47. Sci Rep. 2016;6:19684 [PubMed: 26813769]

36. Frangogiannis NG, Ren G, Dewald O, Zymek P, Haudek S, Koerting A, Winkelmann K, Michael LH, Lawler J, Entman ML. Critical role of endogenous thrombospondin-1 in preventing expansion of healing myocardial infarcts. Circulation. 2005;111:2935–2942 [PubMed: 15927970]

37. Wang S, Sorenson CM, Sheibani N. Lack of thrombospondin 1 and exacerbation of choroidal neovascularization. Arch Ophthalmol. 2012;130:615–620 [PubMed: 22232368]

38. Brew K, Nagase H. The tissue inhibitors of metalloproteinases (timps): An ancient family with structural and functional diversity. Biochim Biophys Acta. 2010;1803:55–71 [PubMed: 20080133]

39. Serra R, Al-Saidi AG, Angelov N, Nares S. Suppression of lps-induced matrix-metalloproteinase responses in macrophages exposed to phenytoin and its metabolite, 5-(p-hydroxyphenyl-), 5-phenylhydantoin. J Inflamm (Lond). 2010;7:48 [PubMed: 20843335]

40. Simpson KS, Komar CM, Curry TE, Jr. Localization and expression of tissue inhibitor of metalloproteinase-4 in the immature gonadotropin-stimulated and adult rat ovary. Biol Reprod. 2003;68:214–221 [PubMed: 12493716]

41. John AS, Hu X, Rothman VL, Tuszynski GP. Thrombospondin-1 (tsp-1) up-regulates tissue inhibitor of metalloproteinase-1 (timp-1) production in human tumor cells: Exploring the functional significance in tumor cell invasion. Exp Mol Pathol. 2009;87:184–188 [PubMed: 19747478]

42. Fei P, Zaitoun I, Farnoodian M, Fisk DL, Wang S, Sorenson CM, Sheibani N. Expression of thrombospondin-1 modulates the angioinflammatory phenotype of choroidal endothelial cells. PLoS One. 2014;9:e116423 [PubMed: 25548916]

43. Akool el S, Doller A, Muller R, Gutwein P, Xin C, Huwiler A, Pfeilschifter J, Eberhardt W. Nitric oxide induces timp-1 expression by activating the transforming growth factor beta-smad signaling pathway. J Biol Chem. 2005;280:39403–39416 [PubMed: 16183640]

44. Zheng X, Xu M, Yao B, Wang C, Jia Y, Liu Q. Il-6/stat3 axis initiated cafs via up-regulating timp-1 which was attenuated by acetylation of stat3 induced by pcaf in hcc microenvironment. Cell Signal. 2016;28:1314–1324 [PubMed: 27297362]

45. Annabi B, Shedid D, Ghosn P, Kenigsberg RL, Desrosiers RR, Bojanowski MW, Beaulieu E, Nassif E, Moumdjian R, Beliveau R. Differential regulation of matrix metalloproteinase activities in abdominal aortic aneurysms. J Vasc Surg. 2002;35:539–546 [PubMed: 11877705]

46. Bumdelger B, Kokubo H, Kamata R, Fujii M, Ishida M, Ishida T, Yoshizumi M. Induction of timp1 in smooth muscle cells during development of abdominal aortic aneurysms. Hiroshima J Med Sci. 2013;62:63–67 [PubMed: 24279124]

47. Eskandari MK, Vijungco JD, Flores A, Borensztajn J, Shively V, Pearce WH. Enhanced abdominal aortic aneurysm in timp-1-deficient mice. J Surg Res. 2005;123:289–293 [PubMed: 15680392]

48. Silence J, Collen D, Lijnen HR. Reduced atherosclerotic plaque but enhanced aneurysm formation in mice with inactivation of the tissue inhibitor of metalloproteinase-1 (timp-1) gene. Circ Res. 2002;90:897–903 [PubMed: 11988491]

49. Lemaitre V, Soloway PD, D'Armiento J. Increased medial degradation with pseudo-aneurysm formation in apolipoprotein e-knockout mice deficient in tissue inhibitor of metalloproteinases-1. Circulation. 2003;107:333–338 [PubMed: 12538437]

50. Allaire E, Forough R, Clowes M, Starcher B, Clowes AW. Local overexpression of timp-1 prevents aortic aneurysm degeneration and rupture in a rat model. J Clin Invest. 1998;102:1413–1420 [PubMed: 9769334]

51. Qian X, Wang TN, Rothman VL, Nicosia RF, Tuszynski GP. Thrombospondin-1 modulates angiogenesis in vitro by up-regulation of matrix metalloproteinase-9 in endothelial cells. Exp Cell Res. 1997;235:403–412 [PubMed: 9299165]

52. Xing C, Arai K, Park KP, Lo EH. Induction of vascular endothelial growth factor and matrix metalloproteinase-9 via cd47 signaling in neurovascular cells. Neurochem Res. 2010;35:1092–1097 [PubMed: 20364320]

53. Hayashido Y, Nakashima M, Urabe K, Yoshioka H, Yoshioka Y, Hamana T, Kitano H, Koizumi K, Okamoto T. Role of stromal thrombospondin-1 in motility and proteolytic activity of oral squamous cell carcinoma cells. Int J Mol Med. 2003;12:447–452 [PubMed: 12964017]

54. Qian X, Rothman VL, Nicosia RF, Tuszynski GP. Expression of thrombospondin-1 in human pancreatic adenocarcinomas: Role in matrix metalloproteinase-9 production. Pathol Oncol Res. 2001;7:251–259 [PubMed: 11882904]

55. Albo D, Shinohara T, Tuszynski GP. Up-regulation of matrix metalloproteinase 9 by thrombospondin 1 in gastric cancer. J Surg Res. 2002;108:51–60 [PubMed: 12443715]

56. Gonzalez-Quesada C, Cavalera M, Biernacka A, Kong P, Lee DW, Saxena A, Frunza O, Dobaczewski M, Shinde A, Frangogiannis NG. Thrombospondin-1 induction in the diabetic

myocardium stabilizes the cardiac matrix in addition to promoting vascular rarefaction through angiopoietin-2 upregulation. Circ Res. 2013;113:1331–1344 [PubMed: 24081879]

57. Moura R, Tjwa M, Vandervoort P, Cludts K, Hoylaerts MF. Thrombospondin-1 activates medial smooth muscle cells and triggers neointima formation upon mouse carotid artery ligation. Arterioscler Thromb Vasc Biol. 2007;27:2163–2169 [PubMed: 17761938]

58. Gandhi NB, Su Z, Zhang X, Volpe EA, Pelegrino FS, Rahman SA, Li DQ, Pflugfelder SC, de Paiva CS. Dendritic cell-derived thrombospondin-1 is critical for the generation of the ocular surface th17 response to desiccating stress. J Leukoc Biol. 2013;94:1293–1301 [PubMed: 23983225]

59. Shi J, Hua L, Harmer D, Li P, Ren G. Cre driver mice targeting macrophages. Methods Mol Biol. 2018;1784:263–275 [PubMed: 29761406]

60. Eliason JL, Hannawa KK, Ailawadi G, Sinha I, Ford JW, Deogracias MP, Roelofs KJ, Woodrum DT, Ennis TL, Henke PK, Stanley JC, Thompson RW, Upchurch GR, Jr. Neutrophil depletion inhibits experimental abdominal aortic aneurysm formation. Circulation. 2005;112:232–240 [PubMed: 16009808]

Highlights

- Inflammatory macrophages are the major source of Thrombospondin-1 (TSP1) elevation in abdominal aortic aneurysm (AAA).

- TSP1 promotes macrophage infiltration by inhibiting TIMP1 expression.

- Myeloid-specific deletion of TSP1 inhibits $CaCl_2$ induced AAA formation.
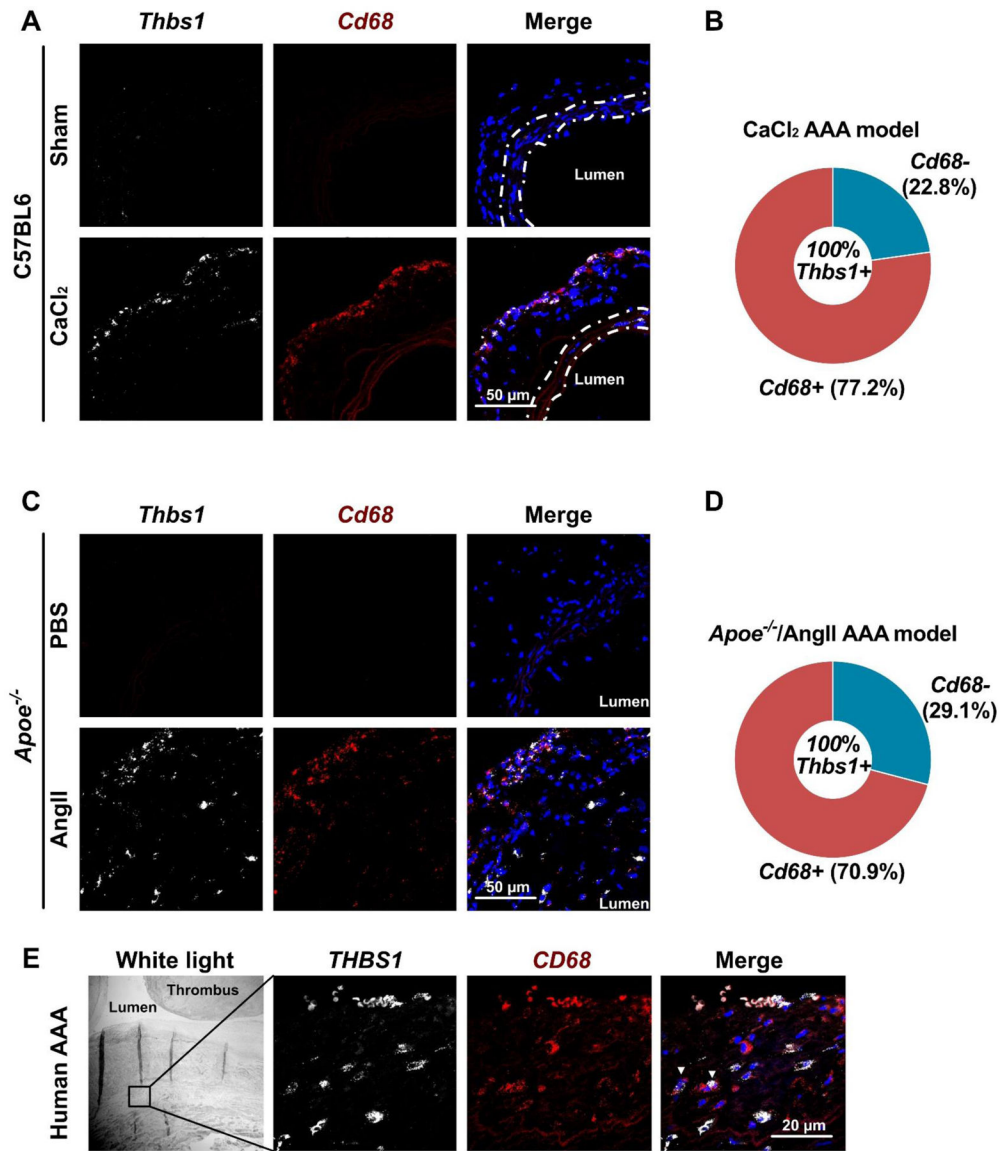
Figure 1. Macrophages (Mφs) are the major source of elevated *Thbs1* expression in abdominal aortic aneurysm (AAA).
(**A-D**) RNA fluorescent *in situ* hybridization (RNA-FISH) of *Thbs1* and *Cd68* on aortic tissue sections 4 days after AAA induction by CaCl$_2$ (A&B) and 7 days after AAA induction by Angiotensin II (C&D), respectively. Representative images and quantifications were shown in (A&C) and (B&D), respectively. n=4 for each group. (**E**) RNA-FISH of *THBS1* and *CD68* expression on human AAA samples. Representative images from three independent samples were shown.
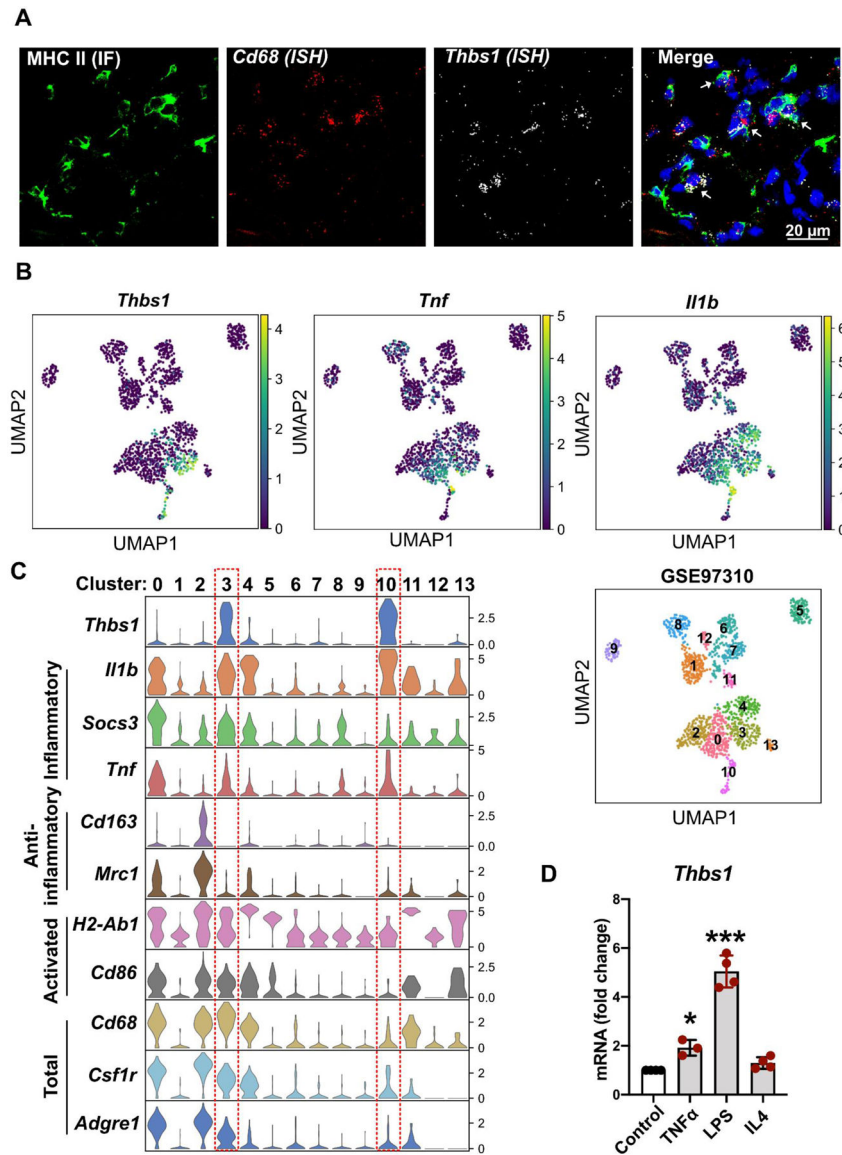
Figure 2. *Thbs1*-expressing macrophages (Mφs) are pro-inflammatory.
(A) RNA fluorescent *in situ* hybridization (RNA-FISH, ISH) of *Thbs1* and *Cd68* combined with immunofluorescent staining (IF) of class II major histocompatibility complex (MHC II) on mouse aortic tissue sections 4 days after AAA induction by $CaCl_2$. **(B)** Analysis of data set GSE97310 in Gene Expression Omnibus followed by Uniform Manifold Approximation and Projection (UMAP2) visualization of *Thbs1*, *Tnf*, *Il2b* and cell clusters in total *Cd45*+ leukocytes from the aortas of male *Ldlr*$^{-/-}$ mice fed with a chow diet for 11 weeks. **(C)** Violin plot of *Thbs1* and indicated Mφ associated genes in cell clusters from (B). **(D)** Mouse bone marrow derived macrophages (BMDMs) were stimulated with TNFα (20 ng/ml), LPS (100 ng/ml) or IL4 (20 ng/ml) for 4 hours. Levels of *Thbs1* mRNA were determined by Real-time PCR. Data were presented as mean ± SD of at least three independent experiments. One-way ANOVA was performed. *$p<0.05$, ***$p<0.001$.
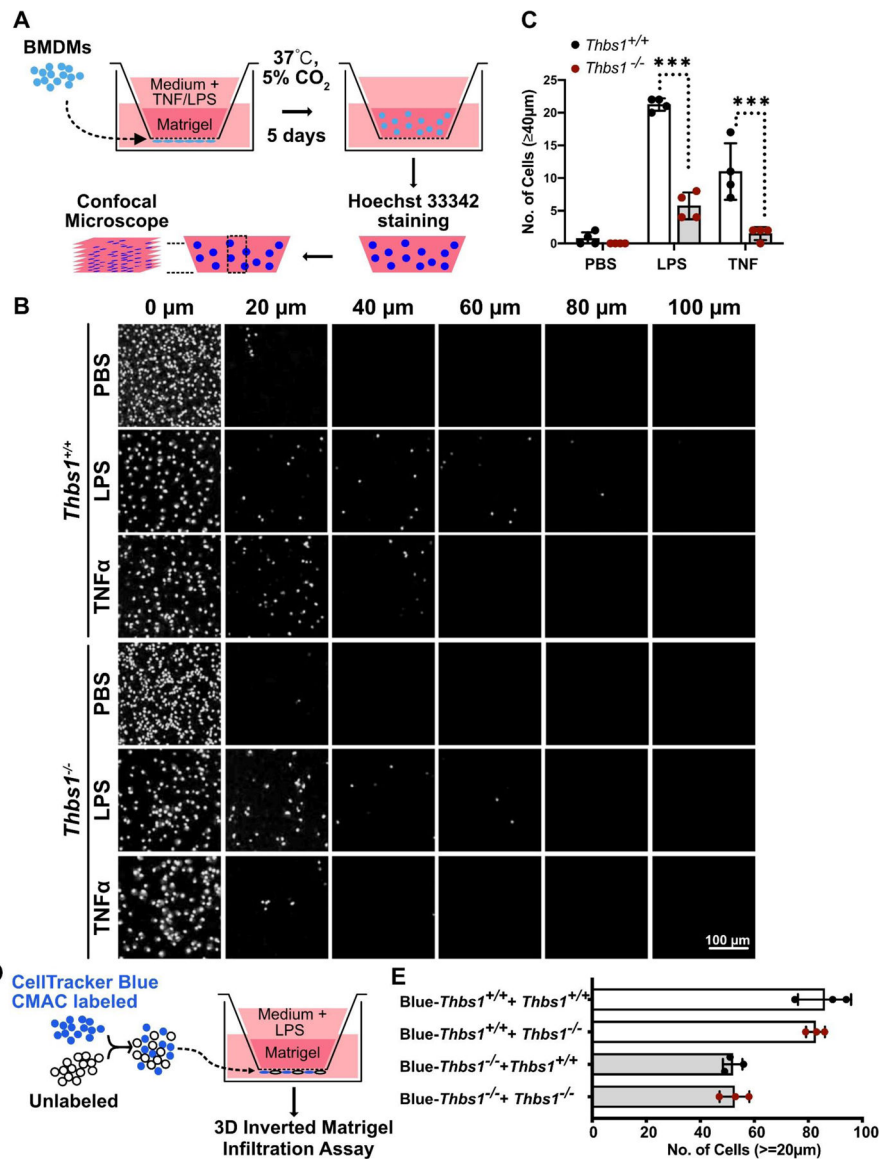
Figure 3. Thrombospondin-1 (TSP1) is necessary for effective macrophage (Mφ) infiltration into extracellular matrix (ECM).
(A) Schematics of 3D Inverted Matrigel Infiltration assay. **(B)** Representative images of indicated optical planes in 3D Inverted Matrigel Infiltration assay. The bottom of the Matrigel was set to 0 μm and a total of 120 μm thick Matrigel was scanned (from bottom to top) for each group. Pictures were captured every 20 μm. LPS: 100 ng/ml, TNFα: 20 ng/ml. **(C)** Quantification of total cell numbers on ≥40 μm planes for each group. **(D)** Schematics of rescue assay. Mφs were prelabeled with CellTracker Blue CMAC dye, then mixed with equal number of unlabeled Mφs. Cell mixture were seeded onto the underside of the Transwell inserts, 100 ng/mL LPS was applied to the upper Transwell chamber. After 5 days, cells migrated into the Matrigel were examined by confocal microscopy without additional staining. **(E)** Quantification of total cell numbers on ≥20 μm planes for each group. Data were presented as mean ± SD of at least three independent experiments. Two-way ANOVA followed by post hoc multiple comparisons were performed. ***p<0.001.
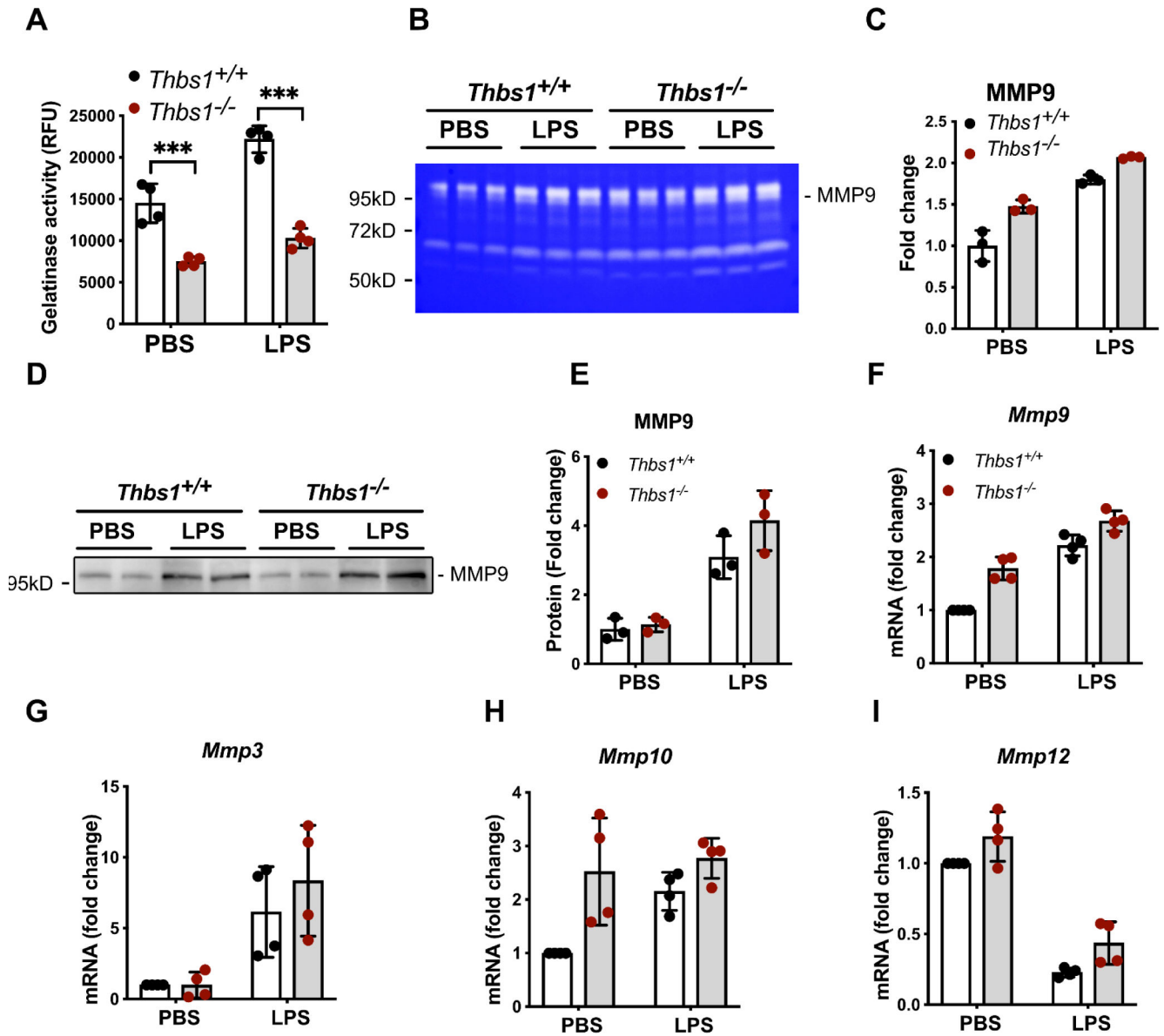
Figure 4. Effects of *Thbs1* gene deficiency on gelatinase activity and matrix metalloproteinase (MMP) expressions.

(A-E) Bone marrow derived macrophages (BMDMs), isolated from *Thbs1*$^{+/+}$ and *Thbs1*$^{-/-}$ mice, were treated with LPS for 24 hours. Gelatinase activities in conditioned medium was evaluated by solution-based fluorometric assay (A). Gel zymography of conditioned medium and quantification of MMP9 activities were shown in (B) and (C), respectively. Protein level of MMP9 in conditioned medium was determined by Western blotting (D&E). A representative blot was shown in (D) and quantification of MMP9 protein levels in (E). (F-I) mRNA levels of *Mmp9*, *3, 10* and *12* in wildtype and *Thbs1*$^{-/-}$ BMDMs were determined by Real-time PCR. Cell were treated with LPS for 4 hours. LPS: 100 ng/ml. Data were presented as mean ± SD of at least three independent experiments. Two-way ANOVA followed by post hoc multiple comparisons was performed. ***p<0.001.
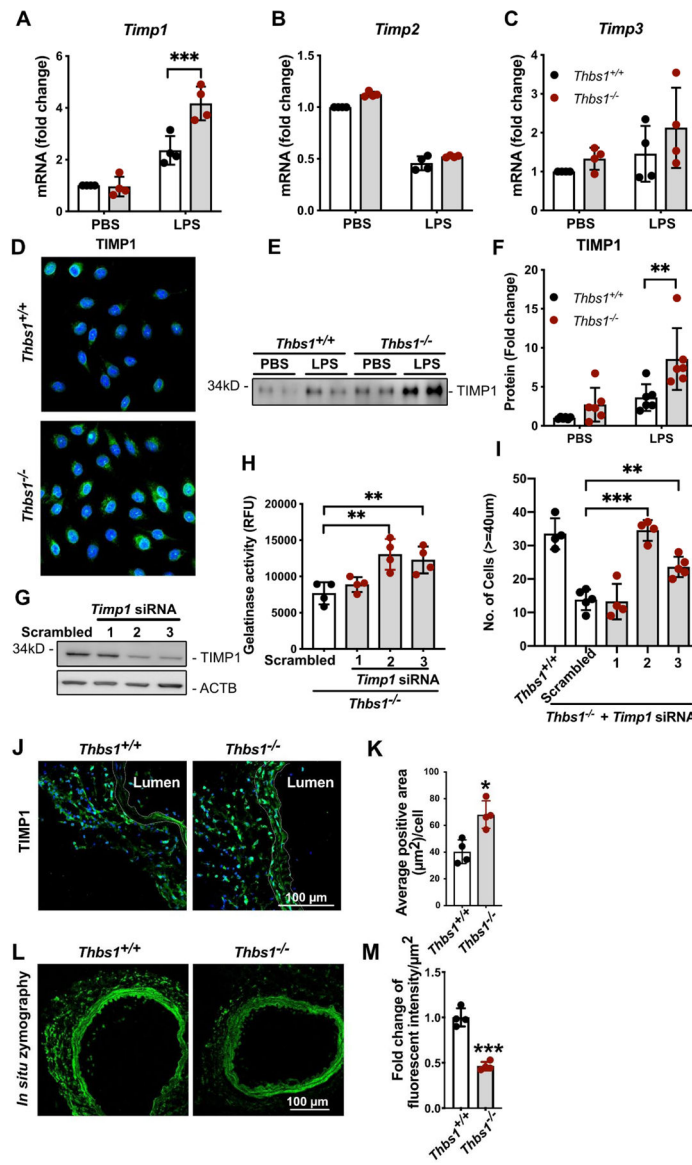
Figure 5. Tissue inhibitor of metalloproteinases-1 (TIMP1) is upregulated in *Thbs1* deficient bone marrow derived macrophages (BMDMs) and aorta.
(A-C) *Thbs1*^{+/+} and *Thbs1*^{−/−} BMDMs were treated with LPS for 4 hours. mRNA levels of *Timp1, 2* and *3* in BMDMs were determined by Real-time PCR. **(D)** BMDMs treated with LPS for 24 hours and stained with anti-TIMP1. **(E&F)** Western blot analysis of TIMP1 in condition medium from BMDMs treated with LPS for 24 hours. A representative blot and quantification were shown in E and F, respectively. **(G)** Validation of *Timp1* siRNA silencing efficiency in wildtype BMDMs by Western blot. **(H)** Solution-based gelatinase activity assay of condition medium from *Thbs1*^{−/−} BMDMs transfected with scrambled siRNA or *Timp1* siRNAs. **(I)** 3D inverted Matrigel infiltration assay of *Thbs1*^{+/+} as well as *Thbs1*^{−/−} BMDMs transfected with indicated *Timp1* siRNAs. LPS: 100 ng/ml. **(J-M)** *Thbs1*^{+/+} and *Thbs1*^{−/−} mice were subjected to AAA induction by $CaCl_2$ (n=4 for each group). Aortic sections were prepared 4 days after surgery and analyzed for TIMP1 levels by immunostaining (J&K), gelatinase activities by *in situ* zymography (L&M). Representative

images and quantifications are shown in (J&L) and (K&M), respectively. Area between dotted lines are medial layer. Data were presented as mean ± SD of at least three independent experiments. Two-way ANOVA followed by post hoc multiple comparisons was performed in A-C and F. One-way ANOVA was performed in H and I. Two-tailed Student's t test was performed in K and M. *p<0.05, **p<0.01, ***p<0.001.
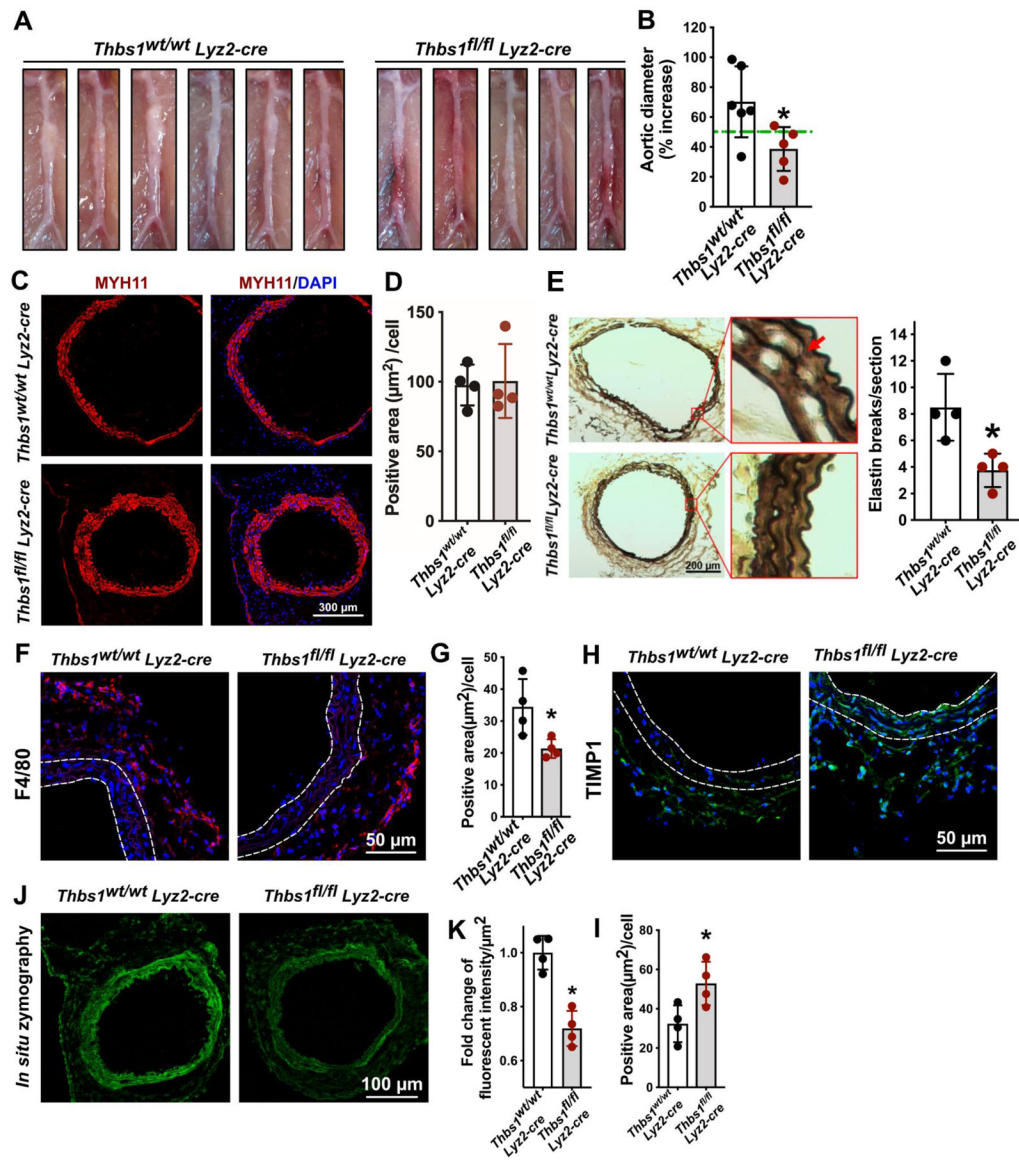
Figure 6. Myeloid-specific *Thbs1* deficiency attenuates abdominal aortic aneurysm (AAA) and macrophage (Mφ) accumulation.

(A) Photos of abdominal aortae taken 28 days after AAA induction by $CaCl_2$. **(B)** Percentage increase of maximal external aortic diameter. An AAA was defined as a percentage increase in aortic diameter 50% (green dashed line) compared to aortic diameter before $CaCl_2$ treatment. *Thbs1$^{wt/wt}$ Lyz2-cre*, n=6; *Thbs1$^{fl/fl}$ Lyz2-cre*, n=5. **(C)** Immunostaining of smooth muscle contractile protein myosin heavy chain 11 (MYH11) on aortic cross sections 4 days after AAA induction by $CaCl_2$. DAPI was used to stain nuclei. **(D)** Quantification of MYH11 positive area in the medial layer relative to total cell number in the medial layer in (C). **(E)** Representative pictures of Elastic stain alongside quantification of averaged elastin breaks per section in aortic cross sections harvested 28 days after AAA induction. Red arrow indicated elastin break. **(F-I)** Immunostaining of F4/80 (F) and tissue inhibitor of metalloproteinases-1 (TIMP1) (H) on aortic cross sections 4 days after AAA induction by $CaCl_2$, respectively. (G) is the quantification of (F). (I) is the
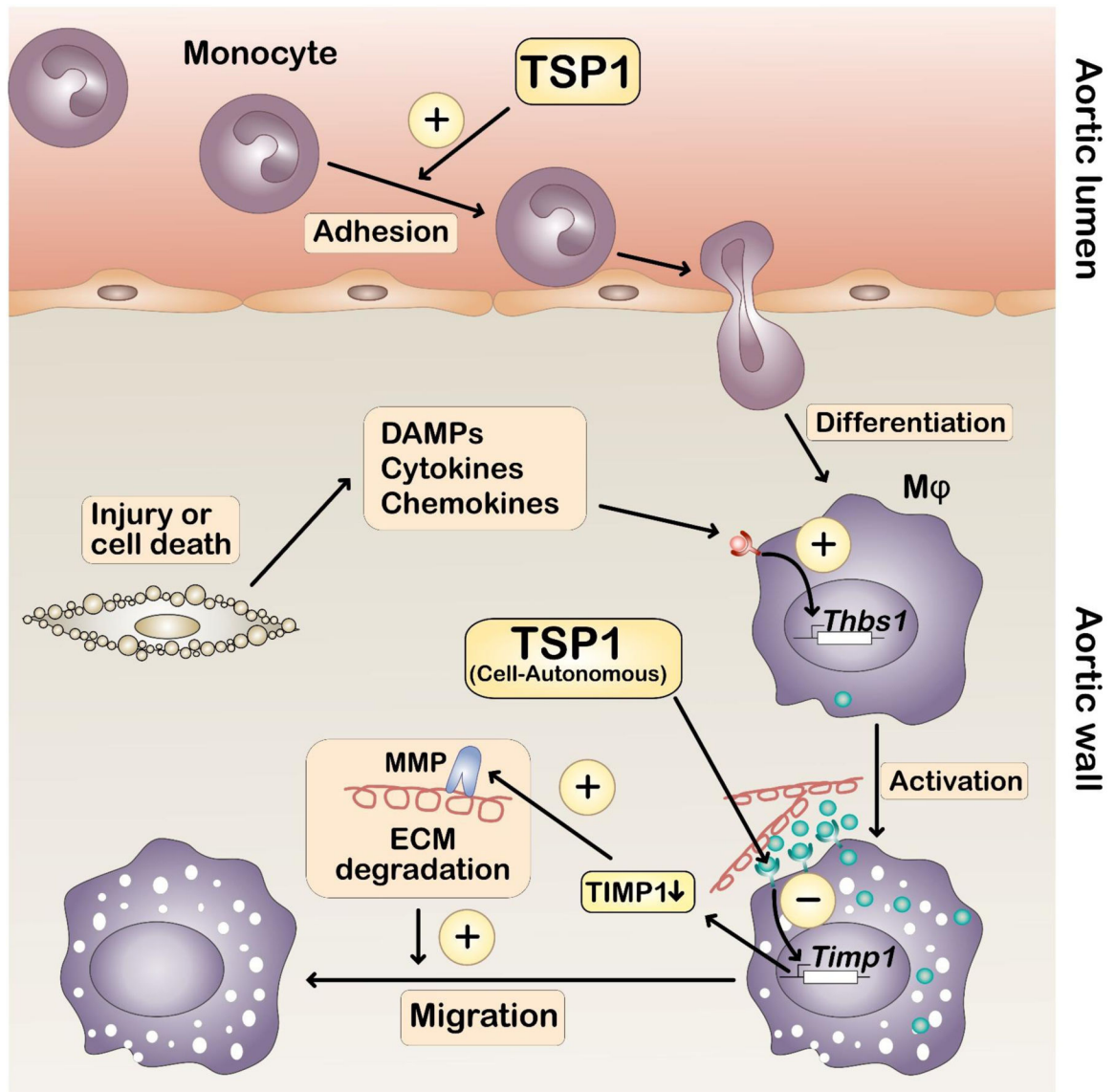
quantification of (H). **(J&K)** *In situ* zymography (J) and quantification (K) on aortic cross sections 4 days after AAA induction by $CaCl_2$. n=4 for each group in C-K. Data were presented as mean ± SD. Two-tailed Student's t test was performed. *p<0.05.

Figure 7. Proposed roles of macrophage (Mφ)-derived thrombospondin-1 (TSP1) in pathophysiology of abdominal aortic aneurysm (AAA).

Major pathophysiological features including extracellular matrix (ECM) degradation, immune cell infiltration, and smooth muscle cell (SMC) death are shown. Cytokines, chemokines, and damage-associated molecular patterns (DAMPs) produced by injured/dying SMCs propel Mφs to an inflammatory state that is associated with higher *Thbs1* expression. Elevated TSP1 suppresses tissue inhibitor of metalloproteinases-1 *(Timp1)* expression by Mφs in a cell-autonomous manner, which subsequently enables matrix metalloproteinases (MMPs) activation, ECM degradation and tissue infiltration. Additionally, TSP1 promotes monocyte adhesion and migration into the vascular wall. Both processes may contribute to vascular inflammation during AAA development.